

Patterning of Non-Linear Optical Crystals in Glass by Laser-Induced Crystallization

T. Komatsu,[†] R. Ihara, T. Honma, and Y. Benino

Department of Materials Science and Technology, Nagaoka University of Technology, Kamitomioka-cho, Nagaoka, Japan

R. Sato

Department of Materials Science and Technology, Tsuruoka National College of Technology, Tsuruoka, Japan

H.G. Kim

Busan Center, Korea Basic Science Institute (KBSI), Busan, Korea

T. Fujiwara

Department of Applied Physics, Graduate School of Engineering, Tohoku University, Aoba, Sendai, Japan

This paper reports recent progress in the patterning of non-linear optical crystals on the glass surface by laser irradiation. Two techniques for the writing of crystal lines have been developed, i.e., rare-earth (samarium) atom heat processing and transition metal atom heat processing, in which a continuous wave Nd:YAG laser (wavelength: $\lambda = 1064$ nm) is irradiated to the glasses containing rare-earth (RE: Sm^{3+} , Dy^{3+}) ions or transition metal (TM: Ni^{2+} , Fe^{2+} , V^{4+}) ions. The writing of crystal lines such as $\beta\text{-BaB}_2\text{O}_4$, $\text{Sm}_x\text{Bi}_{1-x}\text{BO}_3$, and $\text{Ba}_2\text{TiGe}_2\text{O}_8$ showing second harmonic generations has been successful. It is clarified from the azimuthal dependence of second harmonic intensity and polarized micro-Raman scattering spectra that crystal lines consist of highly oriented crystals along the crystal line growth direction. It is also possible to write two-dimensional crystal bending or curved lines by just changing the laser scanning direction. The mechanism of the laser-induced crystallization has been proposed.

I. Introduction

GLASSES having high transparency, high chemical durability, excellent thermal and electrical properties are key materials in microelectronics, optics, and optical fiber technology. Micro-fabrication of glass materials has found increasingly more applications in optoelectronics, telecommunications, and photonic devices such as optical gratings and waveguides, and laser irradiation to glass has received considerable attention as a new tool of spatially selected micro-fabrication.^{1–5} For instance, a permanent change of refractive index can be induced in Ge-doped SiO_2 optical fibers by ultraviolet laser irradiation to produce Bragg gratings under suitable exposure conditions.¹ In the studies of laser-induced structural modifications of glass reported by many researchers so far, most of the target glasses are SiO_2 -based glasses, source lasers are mainly short-wavelength excimer lasers or femtosecond pulsed lasers, and structural modifications are refractive index changes.

M. Davies—contributing editor

On the other hand, it is well recognized that glass is the material that has an inversion symmetry, in principle, yielding no second-order optical non-linearity or ferroelectricity. This has generally brought glass materials only to passive usage like optical glass fibers, while second-order optical non-linearity is the property absolutely required for active applications such as electro-optic switching and wavelength conversion. From this point of view, it is of importance and interest to design spatially selected patterning of non-linear optical/ferroelectric crystals in glass.

The present authors' group succeeded in writing non-linear optical crystal dots and lines in Sm_2O_3 (Dy_2O_3)-containing glasses by irradiation of a continuous wave (cw) Nd:YAG laser with a wavelength of $\lambda = 1064$ nm.^{6–8} This new technique has been called “rare-earth (samarium) atom heat processing” (designated here as REAH [SAAH] processing) and has been applied to various glass systems.^{9–18} It should be emphasized that Nd:YAG laser is very conventional compared with other kinds of lasers such as ultraviolet or femtosecond pulsed laser. A key point in REAH processing is a combination of rare-earth ions and cw Nd:YAG laser with $\lambda = 1064$ nm, and it is prerequisite to prepare glasses with some amounts (\sim more than 8 mol%) of Sm_2O_3 (or Dy_2O_3) in order to increase the temperature sufficiently in the laser-irradiated region. Considering the concept of REAH processing, other combinations would be possible for laser-induced crystallization in glass.^{19,20} For instance, the present authors' group²⁰ found that the combination of transition (TM) metal ions such as Fe^{2+} , Ni^{2+} , and V^{4+} and cw Nd:YAG laser ($\lambda = 1064$ nm) induces effectively crystallization in glasses with a small amount (\sim 1 mol%) of TM ions. This technique has been proposed to be called “transition metal atom heat (TMAH) processing.”

In this paper, we report recent progress in the patterning of crystal lines showing second-order optical non-linearities on the glass surface by using REAH (SAAH) and TMAH processing. The mechanism of the laser-induced crystallization has also been discussed. It should be emphasized that studies on the patterning (writing) of crystal lines in glass by laser irradiation techniques except REAH and TMAH processing, are a few.^{21,22}

II. REAH/TMAH Processing

In rare-earth atom heat processing, cw Nd:YAG lasers with $\lambda = 1064$ nm are irradiated onto glasses containing Sm_2O_3 (or

Manuscript No. 22095. Received August 9, 2006; approved October 9, 2006.

Presented at the Eighth International Symposium on Crystallization in Glasses and Liquids, Jackson Hole, USA.

[†]Author to whom correspondence should be addressed. e-mail: komatsu@chem.nagaokaut.ac.jp

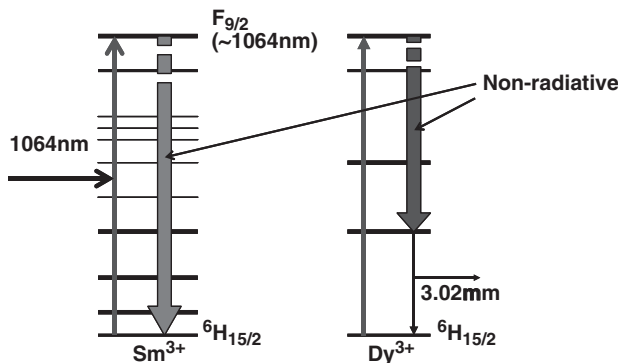


Fig. 1. Electronic energy levels of Sm^{3+} and Dy^{3+} ions.

Dy_2O_3). As Sm^{3+} (or Dy^{3+}) has an absorption band at around 1064 nm, some amounts of cw Nd:YAG laser are absorbed by Sm^{3+} in glass through $f-f$ transitions (${}^6\text{F}_{9/2} \leftarrow {}^6\text{H}_{5/2}$). For example, $10\text{Sm}_2\text{O}_3-40\text{BaO}-50\text{B}_2\text{O}_3$ glass has an absorption coefficient of $\alpha = 7.9 \text{ cm}^{-1}$ at $\lambda = 1064 \text{ nm}$.¹⁰ The electronic energy levels of Sm^{3+} and Dy^{3+} are shown in Fig. 1. As the main relaxation mechanism from ${}^6\text{F}_{9/2}$ to ${}^6\text{H}_{5/2}$ is non-radiative, the YAG laser energy absorbed by Sm^{3+} in glass is transferred to the lattice system (lattice vibrations) through electron-phonon coupling. That is, the surrounding of Sm^{3+} is heated through such a non-radiative relaxation process. Consequently, if the temperature of the laser-irradiated region becomes higher than the glass transition or crystallization temperatures of a given glass, structural modification such as a refractive index change or crystallization could be induced. As the heat dissipation from the laser-irradiated region to the surrounding glass medium is expected to occur rapidly, it would be necessary to irradiate laser continuously to maintain high temperatures (greater than the crystallization temperature) and thus to use continuous-wave type lasers for laser-induced crystallization in glass. It should be emphasized that, in the case of a nanopulse Nd:YAG laser with $\lambda = 1064 \text{ nm}$, no crystallization has been induced in our various studies.^{6-18,23}

It is well known that transition metal ions such as Ni^{2+} and Fe^{2+} in glass give rise to absorption bands in the visible and infra-red spectral regions. As an example, the optical absorption spectra at room temperature for NiO (1 mol%) doped $33.3\text{BaO}-16.7\text{TiO}_2-50\text{GeO}_2$ glass are shown in Fig. 2. The absorption bands around 300–600 and 750–1400 nm are attributed to the ${}^3\text{A}_2 \rightarrow {}^3\text{T}_1$ and ${}^3\text{A}_2 \rightarrow {}^3\text{T}_2$ transition in six-fold Ni^{2+} ions,²⁴ respectively. The absorption coefficient at 1064 nm is $\alpha = 6.01 \text{ cm}^{-1}$ for this NiO-doped glass. It should be pointed out that the value of $\alpha = 6.01 \text{ cm}^{-1}$ in the glass containing only 1 mol% NiO

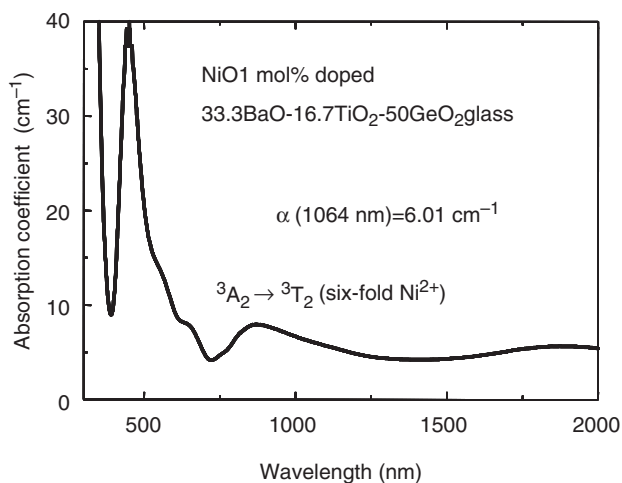


Fig. 2. Optical absorption spectrum at room temperature for the NiO-doped (1 mol%) $33.3\text{BaO}-16.7\text{TiO}_2-50\text{GeO}_2$ glass.

is comparable with those for the glasses with 10 mol% Sm_2O_3 content.¹⁰ It is, therefore, expected that Nd:YAG laser-irradiated spots in NiO-doped glasses would be heated, although the non-radiative relaxation phenomenon of Ni^{2+} ions in glasses, in particular at the ${}^3\text{A}_2 \rightarrow {}^3\text{T}_2$ transition, has not been clarified quantitatively. Indeed, we found that TM ions such as Fe^{2+} , Ni^{2+} , and V^{4+} act as effective atom heaters, consequently, inducing the crystallization in glass by Nd:YAG laser irradiation.²⁰ Inoue *et al.*²⁵ examined the phenomenon of the refractive index change in CoO-doped (2 mol%) TeO_2 -based glasses due to the pulsed laser irradiation with $\lambda = 523 \text{ nm}$ and proposed that the refractive index change (not crystallization) is derived from the change of the fictive temperature of the glasses. Their study also suggests that even in the TMAH processing developed by our research group, the use of cw (not pulsed) Nd:YAG laser is required to induce crystallization.

III. Experimental Procedure

Glasses such as $10\text{Sm}_2\text{O}_3-35\text{Bi}_2\text{O}_3-55\text{B}_2\text{O}_3$, $10\text{Sm}_2\text{O}_3-40\text{BaO}-50\text{B}_2\text{O}_3$, and $33.3\text{BaO}-16.7\text{TiO}_2-50\text{SiO}_2$ (mol%) were prepared by a conventional melt quenching method. Details of the base glass preparation have been described elsewhere.^{6-18,20} The glass transition, T_g , crystallization onset, T_x , and crystallization peak, T_p , temperatures were determined using differential thermal analyses (DTA) at a heating rate of 10 K/min. The quenched glasses were annealed at around T_g to release internal stress and then polished mechanically to obtain a mirror finish with CeO_2 powders.

A cw Nd:YAG laser with $\lambda = 1064 \text{ nm}$ was irradiated to the polished surface of the glasses. The laser beam was focused on the surface of the glasses using an objective lens (magnification 20 or 60) and the sample stage was automatically moved during laser irradiations to construct line patterns. Crystal lines written by Nd:YAG laser irradiation were observed with a polarization optical microscope. The second harmonic intensity of crystal lines was measured by using a fundamental wave of Q-switched pulse Nd:YAG laser with $\lambda = 1064 \text{ nm}$ as a laser source, in which linearly polarized fundamental laser beams were introduced into crystal lines perpendicularly, and the azimuthal dependence of second harmonic generation (SHG) signals was measured by rotating the sample against incident lasers. Polarized micro-Raman-scattering spectra at room temperature for crystal lines written by Nd:YAG laser irradiation were measured with a laser microscope (Tokyo Instruments Co., Tokyo, Japan; Nanofinder) operated at Ar^+ (488 nm) laser.

IV. Results and Discussion

(1) Writing and Features of Crystal Lines

As the YAG laser energy absorbed by Sm^{3+} in glass is transferred to the lattice vibration energy, the temperature of the laser-irradiated region is sensitive to the amount of Sm_2O_3 in a given glass. Under the conditions of the cw Nd:YAG laser power of $< 1 \text{ W}$, Sm_2O_3 contents of over around 8 mol% are needed to induce structural modifications such as refractive index change and crystallization.⁶⁻¹⁸ As an example, the polarization optical micrographs for the sample obtained by Nd:YAG laser irradiation in $10\text{Sm}_2\text{O}_3-35\text{Bi}_2\text{O}_3-55\text{B}_2\text{O}_3$ glass are shown in Fig. 3, where a Nd:YAG laser with powers of $P = 0.6-0.8 \text{ W}$ and a scanning speed of $S = 10 \text{ }\mu\text{m/s}$ was irradiated on the glass surface.¹⁵ At a laser power of $P = 0.6 \text{ W}$, it was found from micro-Raman scattering spectrum that the line is not crystal, but glass, indicating the formation of refractive index change. In $P = 0.66 \text{ W}$, a homogeneous crystal line with a uniform width of $\sim 5 \text{ }\mu\text{m}$ was clearly written. When the laser power is higher than 0.8 W, crystals with a rough morphology grow as shown in Fig. 3. Although the mechanism of the formation of these rough morphologies is unclear, the results suggest the instability of the crystal growth front. That is, the crystal growth behavior similar to the so-called Mullins-Sekerka

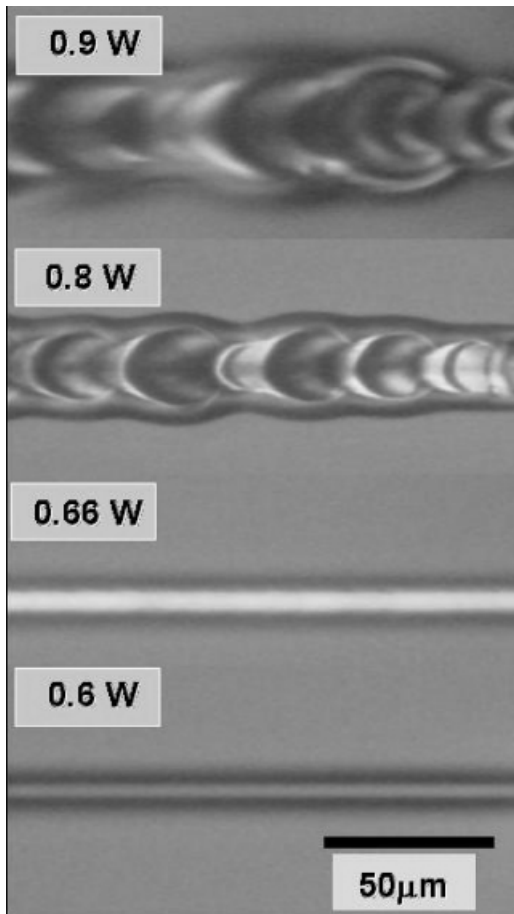


Fig. 3. Polarization optical micrographs for 10Sm₂O₃-35Bi₂O₃-55B₂O₃ sample obtained by Nd:YAG laser irradiation. The laser power was 0.6–0.9 W and the scanning speed was 10 μm/s.

instability²⁶ for the shape of a moving planar liquid–solid interface might occur even in the Nd:YAG laser-induced crystallization in glass.

As 10Sm₂O₃-35Bi₂O₃-55B₂O₃ glass has values of $T_g = 474^\circ\text{C}$ and $T_x = 574^\circ\text{C}$, it is considered that the laser-irradiated regions with powers of >0.65 W would be heated up to temperatures higher than $\sim 580^\circ\text{C}$. The crystalline phase in the laser-irradiated region with a power of 0.66 W shown in Fig. 3 is Sm_xBi_{1-x}BO₃, which is a non-linear optical crystal showing a strong SHG. Indeed, we can observe SHGs from the lines written by YAG laser irradiation.^{8,9,18}

Crystal lines consisting of other non-linear optical crystalline phases have been successfully written in glasses using an REAH processing,^{10,12-14,16,17} e.g., β-BaB₂O₄ crystal lines in Sm₂O₃(Dy₂O₃)-BaO-B₂O₃, KSm(PO₃)₄ crystal lines in K₂O-Sm₂O₃-P₂O₅, β'-Sm₂(MoO₄)₃ crystal lines in Sm₂O₃-MoO₃-B₂O₃, and Sr_{0.5}Ba_{0.5}Nb₂O₆ crystal line in Sm₂O₃-SrO-BaO-Nb₂O₅-B₂O₃ glasses.

The polarization optical micrograph for the cross-section of a crystal line written by Nd:YAG laser irradiation ($P = 0.42$ W, $S = 10$ μm/s) in 21.25Sm₂O₃-63.75MoO₃-15B₂O₃ glass (mol%) with $T_g = 528^\circ\text{C}$ and $T_p = 572^\circ\text{C}$ is shown in Fig. 4. It was confirmed from the micro-Raman scattering spectrum that this crystal line consists of the non-linear optical/ferroelectric β'-Sm₂(MoO₄)₃ crystalline phase.¹⁶ It is seen that β'-Sm₂(MoO₄)₃ crystals grow deeply into the interior of the glass during laser scanning and a swelling occurs at the surface. The formation of swells suggests that a liquid phase is locally formed by Nd:YAG laser irradiation.

As one demonstration for the techniques developed in our group, a famous ground picture (bird) in Nazca (Peru in South America) was designed on the surface of 8Sm₂O₃-37Bi₂O₃-55B₂O₃ glass using Nd:YAG laser irradiation ($P = 0.8$ – 0.9 W,

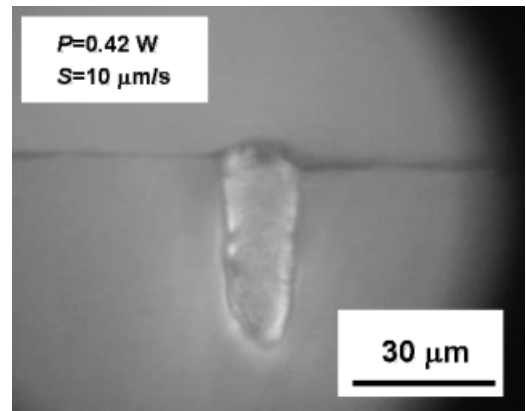


Fig. 4. Polarization optical micrograph for the cross section of a crystal lines written by Nd:YAG laser irradiation in 21.25Sm₂O₃-63.75MoO₃-15B₂O₃ glass. The laser power was 0.42 W and the scanning speed was 10 μm/s.

$S = 4$ μm/s, and the result is shown in Fig. 5. Although the designed picture has various bending angles, a patterning of a bird showing SHGs has been successful.¹⁸

(2) Quality of Crystal Lines

The quality of the crystal lines written by Nd:YAG laser irradiation is very important for application to light control photonic devices. In order to examine the quality of the crystal lines, β-BaB₂O₄ (the so-called β-BBO) crystal lines were selected for the following reasons: β-BBO is one of the most important non-linear optical crystals in laser optics, and its crystal structure is well known. Its remarkable features include a large second-order optical non-linearity of $d_{22} = 2.22$ pm/V and a wide optical transmittance range (190–3500 nm). A crystal-line array of 15 lines was prepared in 10Sm₂O₃-40BaO-50B₂O₃ glass by scanning Nd:YAG laser ($P = 0.6$ W) irradiation with a speed of $S = 5$ μm/s, where the length of each crystal line is 10 mm and the distance between the lines (pitch) is 50 μm.^{10,14} The polarization optical micrograph for such crystal lines is shown in Fig. 6. The XRD pattern for such a crystal-line array is shown in Fig. 7. The peak corresponding to the (110) plane in β-BBO is confirmed, indicating that β-BBO crystals are highly oriented in the lines.

The azimuthal dependence of SHG signals for β-BBO crystal lines is shown in Fig. 8. The maximum SH intensities are observed at the rotation angles of $\sim 0^\circ$ and 180° , and the minimum intensities are located at 90° and 270° . The same experiment was

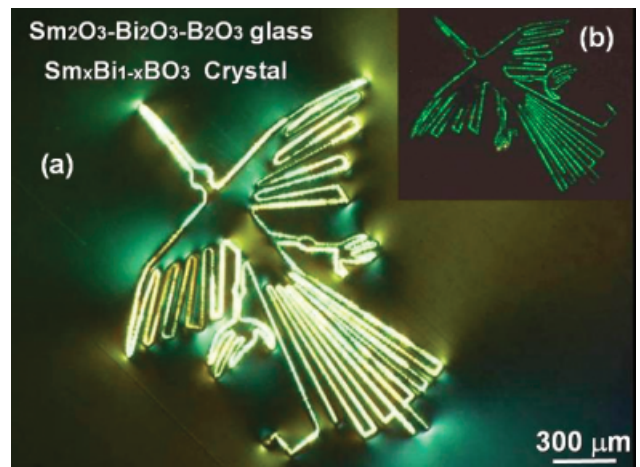


Fig. 5. Polarization optical micrograph (a) and second harmonic generation microscope observation (b) for the curved line (designed as a ground picture (bird) in Nazca) on the surface of glass written by Nd:YAG laser irradiation.

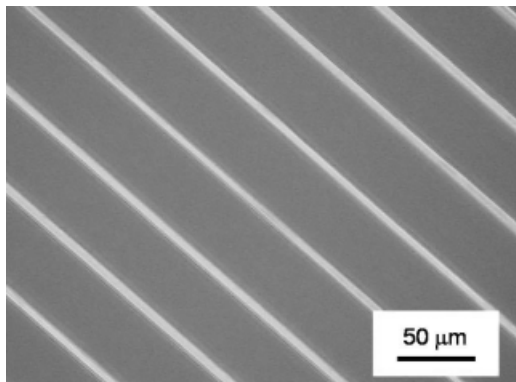


Fig. 6. Polarization optical micrograph for the crystal straight lines written by Nd:YAG laser irradiation in $10\text{Sm}_2\text{O}_3\text{-}40\text{BaO-}50\text{B}_2\text{O}_3$ glass. The laser power was 0.6 W and the scanning speed was $5\ \mu\text{m/s}$.

carried out for the y -cut β -BBO single crystal obtained commercially, and the results are also shown in Fig. 8. The y -cut plane in a β -BBO single crystal corresponds to the (110) plane. It is clear that the azimuthal dependence of SHG signals for β -BBO crystal lines written by Nd:YAG laser irradiation in the glasses is almost the same as that for a commercially available y -cut β -BBO single crystal.¹⁰ We also found that polarized micro-Raman spectra for β -BBO crystal lines are almost the same as those for the y -cut β -BBO single crystal.¹⁴ These results strongly suggest that the crystal lines written by Nd:YAG laser irradiation might be β -BaB₂O₄ single crystals with a c -axis orientation along the laser scanning direction.

The polarization optical micrograph for the sample obtained by Nd:YAG laser irradiation ($P = 0.85\ \text{W}$, $S = 5\ \mu\text{m/s}$) in NiO-doped (1 mol%) $33.3\text{BaO-}16.7\text{TiO}_2\text{-}50\text{GeO}_2$ glass (designated here as BTG50 glass) is shown in Fig. 9. Structural modification with a width of approximately $5\ \mu\text{m}$ is clearly observed in the laser-irradiated region. From the micro-Raman-scattering spectra for the laser-irradiated region, it is demonstrated that fersnoite-type Ba₂TiGe₂O₈ crystals are formed.²⁰ Furthermore, it was confirmed from the azimuthal dependence of SHG signals that Ba₂TiGe₂O₈ crystals are highly oriented along the laser scanning direction.²⁰ The BTG50 glass has values of $T_g = 670$ and $T_x = 780^\circ\text{C}$, and it is, therefore, considered that the temperature of the Nd:YAG laser-irradiated region in NiO-doped BTG50 glass would increase at least up to around 800°C . In other words, a small addition of 1 mol% NiO is effective

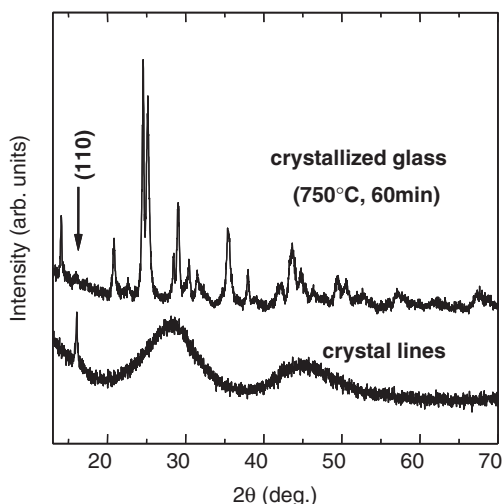


Fig. 7. X-ray diffraction (XRD) pattern for a crystal line array obtained by YAG laser irradiation in $10\text{Sm}_2\text{O}_3\text{-}40\text{BaO-}50\text{B}_2\text{O}_3$ glass. The XRD powder pattern for the crystallized glass obtained by heat treatment in an electric furnace is also shown. The crystalline phase is assigned to β -BaB₂O₄.

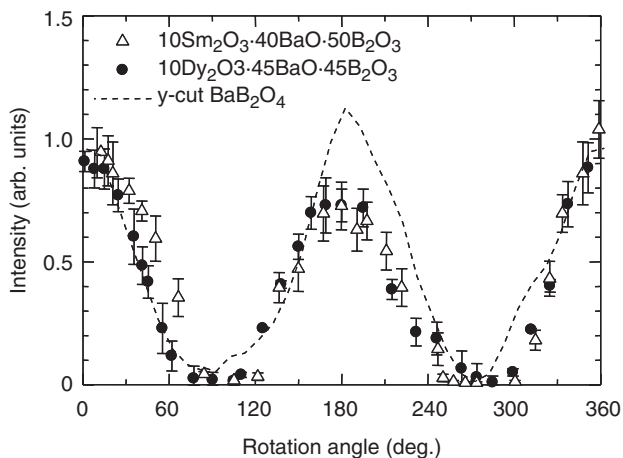


Fig. 8. Azimuthal dependence of second harmonic generation signals for crystal lines written by Nd:YAG laser irradiation in $\text{Sm}_2\text{O}_3\text{-Dy}_2\text{O}_3\text{-BaO-B}_2\text{O}_3$ glasses. The data for a commercially available β -BaB₂O₄ single crystal are also shown.

in the heating of glasses by cw Nd:YAG laser irradiation. It is extremely important to determine the incorporation amount of Ni²⁺ into Ba₂TiGe₂O₈ crystals. The clear observation of SHG (green light of 532 nm) from Ba₂TiGe₂O₈ crystal lines suggests that the incorporation of Ni²⁺ into Ba₂TiGe₂O₈ crystal lines might be small. If a large amount of Ni²⁺ is incorporated, a clear SHG would not be observed because of a strong absorption of the SH waves with $\lambda = 532\ \text{nm}$ due to Ni²⁺.

Similar experiments were carried out for Fe₂O₃- and V₂O₅-doped (0.3–1 mol%) BTG50 glasses,²⁰ and it was found that highly oriented Ba₂TiGe₂O₈ crystal lines are written by Nd:YAG laser irradiations. It is, therefore, concluded that the absorption of the $d-d$ transition of TM ions for a Nd:YAG laser with $\lambda = 1064\ \text{nm}$ is effective in inducing crystallization of glasses. It is known that fersnoite-type Ba₂TiGe₂O₈ crystals reveal interesting dielectric and optical features such as piezoelectricity and ferroelectricity, and in addition, the present authors' group^{27,28} reported that the surface-crystallized glasses consisting of Ba₂TiGe₂O₈ crystals show the large second-order optical non-linearity comparable with that of a LiNbO₃ single crystal. It is, therefore, of interest to write Ba₂TiGe₂O₈ crystal lines on the glass surface by Nd:YAG laser irradiation.

(3) Writing of Bending Crystal Lines

Usually, optical waveguides such as ferroelectric Ti-doped LiNbO₃ single crystals have been fabricated by constructing curved lines (Y-shaped divergence) with different refractive indices in substrates. It is, therefore, of extreme importance to establish techniques for the writing of crystal-curved lines in glass mate-

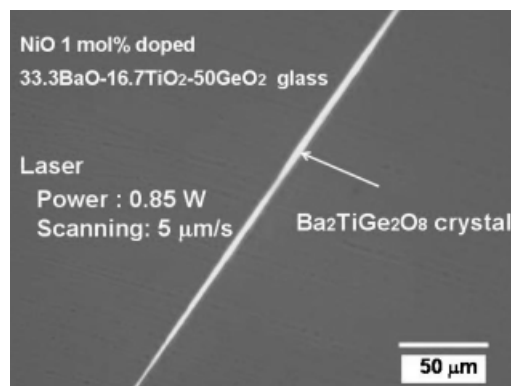


Fig. 9. Polarization optical micrograph for the line written by Nd:YAG laser irradiation in NiO-doped (1 mol%) $33.3\text{BaO-}16.7\text{TiO}_2\text{-}50\text{GeO}_2$ glass.

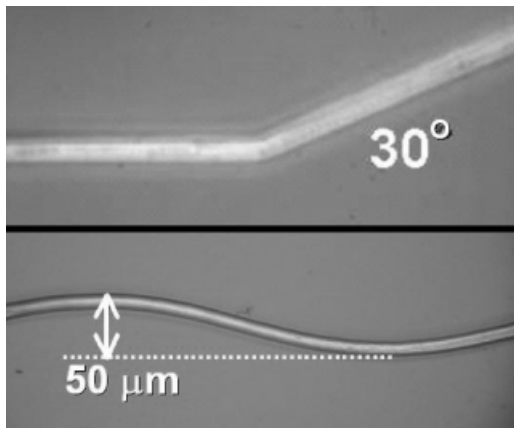


Fig. 10. Polarization optical micrographs for the bending (angle 30°) and sine-shaped lines written by Nd:YAG laser irradiation in $8\text{Sm}_2\text{O}_3\text{-}37\text{Bi}_2\text{O}_3\text{-}55\text{B}_2\text{O}_3$ glass. The laser irradiation conditions are $P = 0.9$ W and $S = 5$ $\mu\text{m/s}$ for the bending line and $P = 0.9$ W and $S = 3$ $\mu\text{m/s}$ for the sine-shaped curved line.

rials, if laser-induced crystal lines are considered for application in active photonic devices such as tunable optical waveguides. The polarization optical micrographs for the bending (angle 30°) and sine-shaped lines written by Nd:YAG laser irradiation in $8\text{Sm}_2\text{O}_3\text{-}37\text{Bi}_2\text{O}_3\text{-}55\text{B}_2\text{O}_3$ glass are shown in Fig. 10. These crystal lines were written by just changing a laser scanning direction, where the laser irradiation conditions are $P = 0.9$ W and $S = 5$ $\mu\text{m/s}$ for the bending line and $P = 0.9$ W and $S = 3$ $\mu\text{m/s}$ for the sine-shaped curved line.¹⁸ The curved crystal lines shown in Fig. 10 consist of non-linear optical $\text{Sm}_x\text{Bi}_{1-x}\text{BO}_3$ crystals.¹⁸ It should be emphasized that any appreciable changes such as structural damages have not been observed even at the bending point.

The polarized micro-Raman scattering spectra for the part located at the behind position of ~ 100 μm from the bending point in the bending crystal line (angle: 30°) are shown in Fig. 11, where the angle between the polarized direction of incident laser and the line growth direction was changed from parallel to perpendicular.¹⁸ In these observations, for instance, the relation with the angle of 60° is designated here as B|P 60° . In the Raman scattering spectra shown in Fig. 11, sharp peaks are observed at 562, 633, and 925 cm^{-1} . These peaks are assigned to $\text{Sm}_x\text{Bi}_{1-x}\text{BO}_3$ crystals showing SHGs.^{29,30} Unfortunately, the crystal structure of the $\text{Sm}_x\text{Bi}_{1-x}\text{BO}_3$ phase has not been clarified at this moment. As can be seen in Fig. 11, the intensity of the peaks at around 1200 cm^{-1} changes largely depending on the angle between the polarized direction of incident laser and the line growth direction. If the crystal line consists of a random assembly of $\text{Sm}_x\text{Bi}_{1-x}\text{BO}_3$ crystals and is thus a polycrystalline line, almost similar Raman scattering spectra would be obtained irrespective of the angle between the polarized direction of incident laser and the line growth direction. That is, the data shown in Fig. 11 suggest that $\text{Sm}_x\text{Bi}_{1-x}\text{BO}_3$ crystals in the behind line from the bending point are highly oriented, as already proposed for the straight crystal lines.⁹

Similar observations were made for the part at the before position of ~ 100 μm from the bending point in the bending crystal line, where the notations such as A|P 60° have been used. It was found that the polarized Raman spectra (i.e., A|P 0° , A|P 30° , A|P 60° , and A|P 90°) at the before position are almost the same as those (Fig. 11) at the behind position.¹⁸ That is, it is suggested that the line after bending also consists of $\text{Sm}_x\text{Bi}_{1-x}\text{BO}_3$ crystals with a high orientation. The relative (normalized) intensities of the peaks at around 1200 cm^{-1} against the peaks at 925 cm^{-1} for the relations of B|P 30° and A|P 30° are shown in Fig. 12. It can be seen that both relations show the same data. Similar behaviors were observed for the relations of B|P 0° and A|P 0° , B|P 60° and A|P 60° , and B|P 90° and A|P 90° . The data shown in Fig. 12 strongly suggest that the crystal plane

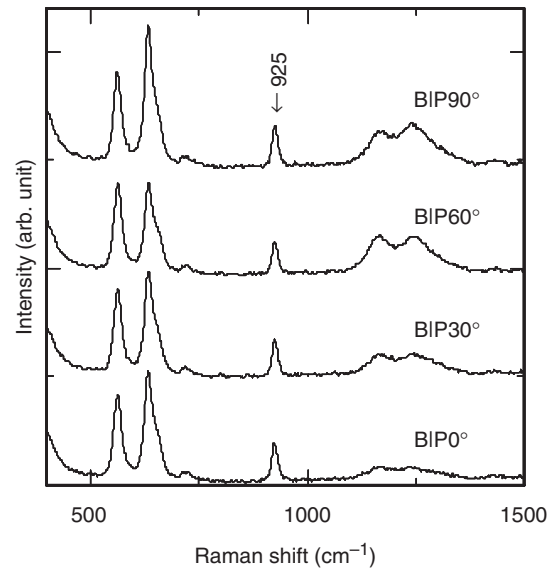
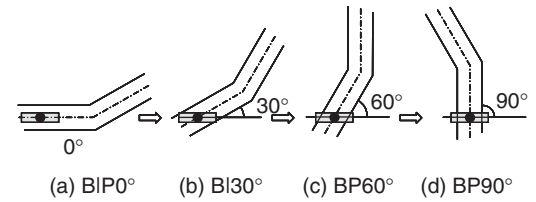


Fig. 11. Polarized micro-Raman scattering spectra for the part located at the behind position of ~ 100 μm from the bending point in the bending crystal line (angle: 30°) written by Nd:YAG laser irradiation in $8\text{Sm}_2\text{O}_3\text{-}37\text{Bi}_2\text{O}_3\text{-}55\text{B}_2\text{O}_3$ glass. The angle between the polarized direction of the incident laser and the line growth direction was changed from perpendicular (B|P 0°) to parallel (B|P 90°).

of $\text{Sm}_x\text{Bi}_{1-x}\text{BO}_3$ crystals to the crystal growth direction might be maintained at positions of over ~ 100 μm from the bending point even after a change in the laser scanning direction. The crystal structure and growth direction at just the bending point are of particular interest, but at this moment we do not have any conclusive data.

The light ($\lambda = 632.8$ nm) transmissions were confirmed for a crystal line (length: 850 μm) with two bending angles of 30° written by Nd:YAG laser irradiation in $8\text{Sm}_2\text{O}_3\text{-}37\text{Bi}_2\text{O}_3\text{-}55\text{B}_2\text{O}_3$ glass, where significant light scattering losses were not observed at the bending points.³¹ These results demonstrate that two-dimensional, highly oriented crystal-curved lines with bending or sine-curved shapes can be successfully written in $\text{Sm}_2\text{O}_3\text{-}Bi_2\text{O}_3\text{-}B_2\text{O}_3$ glasses using REAH (SAAH) processing. If the crystal line consists of a random assembly of crystals, a large scattering of light would occur at the interface between crystals. The quantitative evaluation on the light transmission loss and mode in the highly oriented crystal lines is now under study.

(4) Mechanism of Laser-Induced Crystallization

In the laser-induced crystallization of glass using Nd:YAG laser irradiation, there are two prominent features compared with usual crystallization of glass using an electric furnace: the first one is the volume expansion in the laser-irradiated region, and the second one is the highly oriented crystal growth along the laser scanning direction. These features strongly suggest that a low-viscous super-cooled liquid (or low viscous melt) is formed in the laser-irradiated region. It is considered that laser irradiation gives a rapid temperature increase in the laser-irradiated part, consequently causing the formation of a low-viscous melt within an extremely short period. In the laser scanning experiments for the writing of crystal lines, therefore, it is considered that crystallization occurs through a cooling process from the high-temperature side to the low-temperature side. On the other

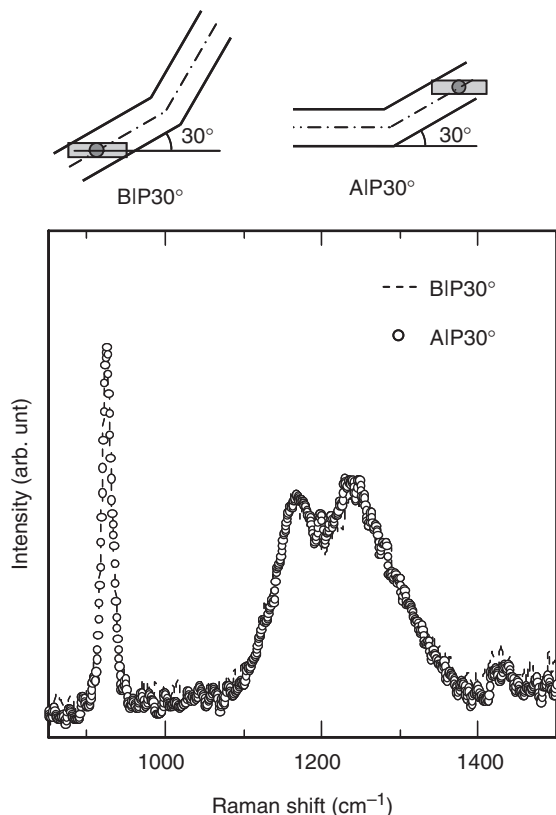


Fig. 12. Polarized micro-Raman scattering spectra for the behind and before positions from the bending point in the bending crystal line (angle: 30°) written by Nd:YAG laser irradiation in $8\text{Sm}_2\text{O}_3\text{-}37\text{Bi}_2\text{O}_3\text{-}55\text{B}_2\text{O}_3$ glass. The relative (normalized) intensities of the peaks at around 1200 cm^{-1} against the peaks at 925 cm^{-1} for the relations of B|P 0° and A|P 0° are plotted.

hand, usual crystallization of glass has been performed through the heating process from the low-temperature side to the high-temperature side. The above consideration (our model) for the crystallization of glass is schematically shown in Fig. 13. Our model suggests that the initial crystalline phase formed in the laser irradiation processing might be different from that formed in the usual crystallization in an electric furnace. The study of the Nd:YAG laser-induced crystallization for the glasses yielding several crystalline phases in usual crystallization is now under consideration in order to confirm our model.

It is important to clarify the spatial and time dependence of the local temperature profile during laser-induced crystalliza-

tion. Considering the heat balance between laser energy absorbed by rare-earth or transition metal ions and heat dissipation from the laser-irradiated region to the surrounding glass medium, the temperature of the laser-irradiated region in glass would depend on the amount of rare-earth or transition metal ions in glass, laser power, laser scanning speed, specific heat, and thermal conductivity of glass. It is difficult to measure directly the temperature of the laser-irradiated region, and thus the estimation of temperature distribution numerically by using a simulation technique such as finite element simulation tools would be useful. Inoue *et al.*²⁵ estimated from a simulation that the maximum temperature of the laser-irradiated spot in CoO-doped TeO_2 -based glasses is becoming higher than the glass transition temperature.

Recently, some studies on laser-induced crystallization of glass using an excimer laser or a femtosecond laser have been reported.^{21,22,32–35} For instance, a periodic structure consisting of an arrangement of ordered nanocrystals has been fabricated in TeO_2 -based glasses through a photo-induced crystallization using XeCl excimer laser ($\lambda = 308\text{ nm}$) irradiation.³² Nogami *et al.*³³ reported the formation of SnO_2 nanoparticles having an average size of 5 nm by irradiation of femtosecond laser pulses with $\lambda = 800\text{ nm}$ in Eu^{3+} -doped $\text{SnO}_2\text{-SiO}_2$ glasses. Yonezaki *et al.*³⁴ also reported the precipitation of non-linear optical crystalline phases such as LiNbO_3 by irradiation of tightly focused femtosecond laser pulses with $\lambda = 800\text{ nm}$ in glasses such as $\text{Li}_2\text{O-Nb}_2\text{O}_5\text{-SiO}_2$ glasses. The mechanism for the structural modification in glass by femtosecond pulse laser irradiation has been discussed in various studies, but, at this moment, the contribution of the thermal effect to the structural modification is unclear. In contrast, in rare-earth atom heat processing and transition atom heat processing developed by our research group, the thermal effect is intrinsic for crystallization in glass, meaning the ease of the control of laser-induced crystallization.

The main aim of our study is to write crystal lines on the glass surface by using laser-induced crystallization. But, by controlling the laser power and scanning speed, line writing with refractive index changes (not crystallization) is possible as shown in Fig. 3. Honma *et al.*²³ found that a large decrease ($\sim 3.5\%$) in the refractive index is induced in $10\text{Sm}_2\text{O}_3\text{-}40\text{BaO-}50\text{B}_2\text{O}_3$ glass by YAG laser irradiations (nanosecond pulse and $\lambda = 1064\text{ nm}$). It is also of interest to clarify the feature of refractive index changed lines written by REAH or TMAH processing using a cw Nd:YAG laser.

V. Conclusion

Two techniques for laser-induced crystallization in glass were developed, i.e., REAH processing and TMAH processing, and were applied to some glasses for the patterning of non-linear optical crystals. It was clarified that these techniques are very effective in the writing of highly oriented crystal lines consisting of non-linear optical crystals such as $\beta\text{-BaB}_2\text{O}_4$, $\text{Sm}_x\text{Bi}_{1-x}\text{BO}_3$, and $\text{Ba}_2\text{TiGe}_2\text{O}_8$. It was also clarified that it is possible to write two-dimensional crystal bending or curved lines by just changing the laser scanning direction. The mechanism of the laser-induced crystallization has been proposed. In particular, it was proposed that crystallization occurs through the cooling process from the high-temperature side to the low-temperature side in the laser scanning experiments for the writing of crystal lines. The development of new techniques for laser-induced crystallization indicates that the science and technology of the crystallization in glass are now in new phase, leading to new challenges.

Acknowledgments

This work was supported by the Ministry of Internal Affairs and Communications Strategic Information and Communications R&D Promotion Programs (SCOPE), a Grant-in-Aid for Scientific Research from the Ministry of Education, Science, Sports, Culture, and Technology, Japan, and by the 21st Century Center of Excellence (COE) Program in Nagaoka University of Technology.

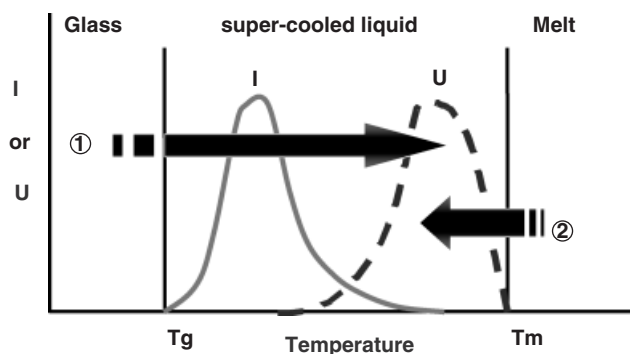


Fig. 13. Model for Nd:YAG laser-induced crystallization in glass. Process ②: in the laser scanning experiments for the writing of crystal lines, crystallization occurs through the cooling process from the high-temperature side to the low-temperature side. Process ①: usual crystallization of glass occurs through the heating process from the low-temperature side to the high-temperature side. I and U are the nucleation and crystal growth rates, respectively.

References

- ¹K. O. Hill, B. Malo, F. Bilodeau, D. C. Jhonson, and J. Albert, "Bragg Grating Fabricated in Monomode Photosensitive Optical Fiber by UV Exposure Through a Phase Mask," *Appl. Phys. Lett.*, **62** [10] 1035–7 (1993).
- ²D. Du, X. Liu, G. Korn, J. Squier, and G. Mourou, "Laser-Induced Breakdown by Impact Ionization in SiO₂ with Pulse Widths from 7 ns to 150 fs," *Appl. Phys. Lett.*, **64** [23] 3071–3 (1994).
- ³K. M. Davis, K. Miura, N. Sugimoto, and K. Hirao, "Writing Waveguides in Glass with a Femtosecond Laser," *Opt. Lett.*, **21** [21] 1729–31 (1996).
- ⁴T. Fujiwara, T. Nakamoto, T. Honma, Y. Benino, and T. Komatsu, "Refractive Index Change Induced by Ultraviolet Laser Irradiations in Erbium-Doped Tellurite Glasses," *Electron. Lett.*, **39** [22] 1576–7 (2003).
- ⁵H. Ebendorff-Heidepriem, "Laser Writing of Waveguides in Photosensitive Glasses," *Opt. Mater.*, **25**, 109–15 (2004).
- ⁶R. Sato, Y. Benino, T. Fujiwara, and T. Komatsu, "YAG Laser-Induced Crystalline Dot Patterning in Samarium Tellurite Glasses," *J. Non-Cryst. Solids*, **289**, 228–32 (2001).
- ⁷T. Honma, Y. Benino, T. Fujiwara, R. Sato, and T. Komatsu, "New Optical Nonlinear Crystallized Glasses and YAG Laser-Induced Crystalline Dot Formation in Rare-Earth Bismuth Borate System," *Opt. Mater.*, **20**, 27–33 (2002).
- ⁸T. Honma, Y. Benino, T. Fujiwara, R. Sato, and T. Komatsu, "Optical Nonlinear Crystalline Dot and Line Patterning in Samarium Bismuth Borate Glasses by YAG Laser Irradiation," *J. Ceram. Soc. Jpn.*, **110** [5] 398–402 (2002).
- ⁹T. Honma, Y. Benino, T. Fujiwara, T. Komatsu, and R. Sato, "Nonlinear Optical Crystal-Line Writing in Glass by Yttrium Aluminum Garnet Laser Irradiation," *Appl. Phys. Lett.*, **82** [6] 892–4 (2003).
- ¹⁰T. Honma, Y. Benino, T. Fujiwara, R. Sato, and T. Komatsu, "Technique for Writing of Nonlinear Optical Single-Crystal Lines in Glass," *Appl. Phys. Lett.*, **83** [14] 2796–8 (2003).
- ¹¹S. Kawasaki, T. Honma, Y. Benino, T. Fujiwara, R. Sato, and T. Komatsu, "Writing of Crystal-Dots and Lines by YAG Laser Irradiation and Their Morphologies in Samarium Tellurite Glasses," *J. Non-Cryst. Solids*, **325**, 61–9 (2003).
- ¹²H. Tanaka, T. Honma, Y. Benino, T. Fujiwara, and T. Komatsu, "YAG Laser-Induced β -BaB₂O₄ Crystalline Dot Formation in Sm₂O₃-BaO-B₂O₃ Glasses," *J. Phys. Chem. Solids*, **64**, 1179–84 (2003).
- ¹³M. Saito, T. Honma, Y. Benino, T. Fujiwara, and T. Komatsu, "Formation of Nonlinear Optical KSm(PO₃)₄ Crystals in Phosphate Glasses by YAG Laser Irradiation," *Solid State Sci.*, **6**, 1013–8 (2004).
- ¹⁴T. Honma, Y. Benino, T. Fujiwara, R. Sato, and T. Komatsu, "Micro-Raman and Photoluminescence Spectra of Sm³⁺-Doped β -BaB₂O₄ Crystal Lines Written by YAG Laser Irradiation in Glass," *J. Phys. Chem. Solids*, **65**, 1705–10 (2004).
- ¹⁵T. Honma, Y. Benino, T. Fujiwara, and T. Komatsu, "Crystalline Phases and YAG Laser-Induced Crystallization in Sm₂O₃-Bi₂O₃-B₂O₃ Glasses," *J. Am. Ceram. Soc.*, **88** [4] 989–92 (2005).
- ¹⁶M. Abe, Y. Benino, T. Fujiwara, T. Komatsu, and R. Sato, "Writing of Nonlinear Optical Sm₂(MoO₄)₃ Crystal Lines at the Surface of Glass by Samarium Atom Heat Processing," *J. Appl. Phys.*, **97**, 123516/1–123516/7 (2005).
- ¹⁷N. Chayapiwut, T. Honma, Y. Benino, T. Fujiwara, and T. Komatsu, "Synthesis of Sm³⁺-Doped Strontium Barium Niobate Crystals in Glass by Samarium Atom Heat Processing," *J. Solid State Chem.*, **178**, 3507–13 (2005).
- ¹⁸R. Ihara, T. Honma, Y. Benino, T. Fujiwara, R. Sato, and T. Komatsu, "Writing of Two-Dimensional Crystal Curved Lines at the Surface of Sm₂O₃-Bi₂O₃-B₂O₃ Glass by Samarium Atom Heat Processing," *Solid State Commun.*, **136**, 273–7 (2005).
- ¹⁹H. Jain, "Transparent Ferroelectric Glass-Ceramics," *Ferroelectrics*, **306**, 111–27 (2004).
- ²⁰T. Honma, Y. Benino, T. Fujiwara, and T. Komatsu, "Transition Metal Atom Heat Processing for Writing of Crystal Lines in Glass," *Appl. Phys. Lett.*, **88**, 231105/1–231105/3 (2006).
- ²¹K. Miura, J. Qiu, T. Mitsuyu, and K. Hirao, "Space-Selective Growth of Frequency-Conversion Crystals in Glasses with Ultrashort Infrared Laser Pulses," *Opt. Lett.*, **25** [6] 408–10 (2000).
- ²²B. Fisette, F. Busque, J. Y. Degorce, and M. Meunier, "Three-Dimensional Crystallization Inside Photosensitive Glasses by Focused Femtosecond Laser," *Appl. Phys. Lett.*, **88**, 091104/1–091104/3 (2006).
- ²³T. Honma, Y. Benino, T. Fujiwara, and T. Komatsu, "Line Patterning with Large Refractive Index Changes in the Deep Inside of Glass by Nanosecond Pulsed YAG Laser Irradiation," *Solid State Commun.*, **135**, 193–6 (2005).
- ²⁴J. S. Berkes and W. B. White, "Optical Spectra of Nickel in Alkali Tetraborate Glasses," *Phys. Chem. Glasses*, **7** [6] 191–9 (1966).
- ²⁵S. Inoue, A. Nukui, K. Yamamoto, T. Yano, S. Shibata, and M. Yamane, "Correlation between Specific Heat and Change of Refractive Index Formed by Laser Spot Heating of Tellurite Glass Surface," *J. Non-Cryst. Solids*, **324**, 133–41 (2003).
- ²⁶W. W. Mullins and R. F. Sekerka, "Stability of a Planar Interface During Solidification of a Dilute Binary Alloy," *J. Appl. Phys.*, **35** [2] 444–51 (1964).
- ²⁷Y. Takahashi, Y. Benino, T. Fujiwara, and T. Komatsu, "Optical Second Order Nonlinearity of Transparent Ba₂TiGe₂O₈ Crystallized Glasses," *Appl. Phys. Lett.*, **81** [2] 223–5 (2002).
- ²⁸Y. Takahashi, Y. Benino, T. Fujiwara, and T. Komatsu, "Large Second-Order Optical Nonlinearities of Fresnoite-Type Crystals in Transparent Surface-Crystallized Glasses," *J. Appl. Phys.*, **95** [7] 3503–8 (2004).
- ²⁹M. J. Pottier, "Mise en Evidence d'un Compose BiBO₃ et de Son Polymorphisme par Spectroscopie Vibratoire," *Bull. Soc. Chim.*, **83** [7–8] 235–8 (1974).
- ³⁰R. Ihara, T. Honma, Y. Benino, T. Fujiwara, and T. Komatsu, "Second-Order Optical Nonlinearities of Metastable BiBO₃ Phases in Crystallized Glasses," *Opt. Mater.*, **27**, 403–8 (2004).
- ³¹R. Ihara, Y. Benino, T. Fujiwara, and T. Komatsu, "Fabrication of Optical Waveguide in Glass by Laser-Induced Crystallization," *Adv. Mater. Res.*, **11–12**, 197–200 (2006).
- ³²T. Fujiwara, R. Ogawa, Y. Takahashi, Y. Benino, T. Komatsu, and J. Nishii, "Laser Induced Photonic Periodic Structure in Tellurite Based Glass Ceramics," *Phys. Chem. Glasses*, **43C**, 213–6 (2002).
- ³³M. Nogami, A. Ohno, and H. You, "Laser-Induced SnO₂ Crystallization and Fluorescence Properties in Eu³⁺-Doped SnO₂-SiO₂ Glasses," *Phys. Rev. B.*, **68**, 104204/1–104204/7 (2003).
- ³⁴Y. Yonezaki, K. Miura, R. Araki, K. Fujita, and K. Hirao, "Space-Selective Precipitation of Non-Linear Optical Crystals Inside Silicate Glasses Using Near-Infrared Femtosecond Laser," *J. Non-Cryst. Solids*, **351**, 885–92 (2005).
- ³⁵B. H. Venkataraman, N. S. Prasad, K. B. R. Varma, V. Rodriguez, M. Maglione, R. Vondermuhll, and J. Etourneau, "Optical Diffraction of Second-Harmonic Signals in the LiBO₂-Nb₂O₅ Glasses Induced by Self-Organized LiNbO₃ Crystallites," *Appl. Phys. Lett.*, **87**, 091113/1–091113/3 (2005). □